

## Article

# The Effect of Bulk Modification of the MF-4SK Membrane with Phosphorylated Hyper-Branched Dendrimer Boltorn H20 on the Mechanisms of Electroconvection/Dissociation of Water and Specific Selectivity to Divalent Ions

Aslan Achoh , Denis Bondarev, Elena Nosova and Stanislav Melnikov \* 

Physical Chemistry Department, Kuban State University, 350040 Krasnodar, Russia; achoh-aslan@mail.ru (A.A.); bondarew.denis1992@gmail.com (D.B.); nosova.el@inbox.ru (E.N.)

\* Correspondence: melnikov.stanislav@gmail.com

**Abstract:** This study focuses on the modification of ion-exchange membranes by incorporating a phosphorylated dendrimer into sulfonated polytetrafluoroethylene membranes to enhance the specific selectivity between mono-/divalent ions, using the  $\text{Ca}^{2+}/\text{Na}^{+}$  pair as an example. This research employs mechanical, physicochemical, and electrochemical analyses to explore the effects of P-H20 incorporation on membrane properties. Bulk modification significantly increases membrane selectivity towards calcium ions (the specific permselectivity coefficient rises from 1.5 to 7.2), while maintaining the same level of the limiting current density. Other findings indicate that bulk modification significantly changes the transport-channel structure of the membrane and alters the mechanism of over-limiting mass transfer. The over-limiting current for the pristine membrane is mainly due to non-equilibrium electroconvection, while modified membranes actively participate in the water-splitting reaction, leading to the suppression of the electroconvection. Despite this drawback, the decrease of the over-limiting potential drop results in a decrease in specific energy consumption from 0.11 to 0.07 kWh/mol. In the underlimiting current mode, the specific energy consumption for all studied membranes remains within the same limits of 0.02–0.03 kWh/mol.

**Keywords:** Boltorn H20; cation-exchange membrane; specific permselectivity; voltammetry; current-voltage characteristic; electroconvection; water splitting



**Citation:** Achoh, A.; Bondarev, D.; Nosova, E.; Melnikov, S. The Effect of Bulk Modification of the MF-4SK Membrane with Phosphorylated Hyper-Branched Dendrimer Boltorn H20 on the Mechanisms of Electroconvection/Dissociation of Water and Specific Selectivity to Divalent Ions. *Electrochem* **2024**, *5*, 84–106. <https://doi.org/10.3390/electrochem5010006>

Academic Editor: Michael Fowler

Received: 5 December 2023

Revised: 10 February 2024

Accepted: 17 February 2024

Published: 20 February 2024



**Copyright:** © 2024 by the authors. Licensee MDPI, Basel, Switzerland. This article is an open access article distributed under the terms and conditions of the Creative Commons Attribution (CC BY) license (<https://creativecommons.org/licenses/by/4.0/>).

## 1. Introduction

The problem of creating ion exchange membranes with pronounced specific selectivity is one of the oldest and most important problems in membrane electrochemistry. Moreover, in recent years, the application of electromembrane systems has been increasing. This has led to a growing need to enhance the selective permeability between counter ions and co-ions, as well as between counter ions with different charges (such as  $\text{Na}^{+}$  and  $\text{Ca}^{2+}$ ) or identical charges (such as  $\text{NO}_3^{-}$  and  $\text{Cl}^{-}$ ). Processes like redox flow batteries, diffusion dialysis, microbial fuel cells, and ion exchange membrane bioreactors demand membranes with high selectivity for distinct counter ions [1].

Within the scope of this study, we will refer to “selectivity” as the preferential transport of one of the ions with the same charge, whereas, typically, the selectivity of an ion-exchange membrane is understood as its ability to transport ions of the same charge sign without differentiation between them. In this sense, ion-exchange membranes can exhibit charge selectivity (based on the magnitude of the charge, for example,  $\text{Li}^{+}$  and  $\text{Mg}^{2+}$ ), as well as specific selectivity (for example, based on the chemical nature of ions with the same charge).

Generally, ion-exchange materials exhibit more pronounced selectivity towards double- and multiple-charged ions [2]. To enhance selectivity towards single-charged ions, studies have been conducted on altering the configuration of the membrane stack [3–5], including

the use of nanofiltration membranes instead of cation-exchange membranes [5]. However, the overwhelming majority of research in this field is dedicated to modifying the properties of ion-exchange membranes through surface modification [6].

Sata et al. extensively investigated the possibilities of modifying ion-exchange membranes to impart selectivity towards monovalent ions and examined the impact of this modification on the resulting characteristics of the electro dialysis process in the 1970s–1980s. These studies were summarized in two reviews dedicated to anion-exchange [7] and cation-exchange [8] membranes. A review [9] compiled patents on methods for obtaining monovalent-selective cation-exchange membranes. The topic of the selectivity of ion-exchange membranes is also briefly discussed in the review by Ran et al. [10] and in detail in the review by Luo et al. [1]. Ge et al. [11] published a monograph on monovalent-selective cation-exchange membranes, focusing on traditional and new methods for obtaining/modifying these membranes. A graph depicting the tradeoff between ion flux and selectivity for several pairs of single-/double-charged cations is presented. In a more general sense, in relation to other membrane processes, this compromise—permeability–selectivity—is well known and widely discussed in the scientific literature, for example in the review [12].

The potential for separating counter ions opens up new directions for the application of electro dialysis, such as selectrodialysis [3] and metathesis electro dialysis [13]. It may also lead to the emergence of new niche applications for electro dialysis, including demineralization of whey [14], extraction of nutrients (particularly phosphorus) from wastewater [15], as well as the production of high-purity casein isolates [16], among others.

A commonly used technique for producing membranes with high selectivity involves depositing a layer of ion polymer with a charge opposite to the charge of the ion-exchange matrix of the membrane substrate onto the membrane-substrate surface [7,8]. The charge of the deposited layer matches the charge of the ions being separated. Recently, there has been a shift towards the deposition of multiple layers, in which the polymer matrix charges alternate [1,11,17,18].

When a layer of ion polymer with a charge opposite to the matrix charge of the membrane substrate is applied onto the later, the ions being separated act as counter ions for the membrane substrate but as co-ions for the modifying layer. Hence, this process will be referred to as co-ion separation. The mechanism of co-ion separation differs somewhat from the process of counter-ion separation. Primarily, in the case of co-ion separation, the main mechanism involves the stronger electrostatic interaction of multi-charged ions with the polymer matrix of the modifying layer, while the physicochemical interaction between ions and the ion-polymer material plays a subordinate role (although it is not entirely excluded). A second difference is the reduction in the magnitude of the limiting current in the electromembrane system, caused by the transition from outer-diffusional kinetics of ion transport to inner-diffusional kinetics [19].

The transition to inner-diffusional kinetics has two significant effects. Firstly, it significantly reduces the current density range in which ion separation is possible. Secondly, it leads to a shift in the operation of the ion-exchange membrane from a “selective mode” to a “water-splitting mode”. In other words, the membrane functions as an asymmetric bipolar membrane. This particular phenomenon was noted by various researchers [17,20,21].

To avoid the transition to the inner-diffusional limiting current while ensuring high specific selectivity of ion-exchange membranes, bulk modification can be employed. In this approach, no charged layers are deposited on the membrane surface. The increase in specific selectivity arises either from the physicochemical interaction of ions with the modifier [22] or from the “reduction” of ionic channels in the transport-channel structure of the membrane, which, in turn, promotes the “sieving effect” [23,24].

Hyperbranched polymers [25] can be a potentially interesting modifying agents, as they provide numerous sites that can be functionalized. Zabolotsky et al. [26] proposed a methodology for obtaining phosphorylated dendrimer Boltorn H20 (referred to as P-H20 hereinafter) and for producing a bilayer (asymmetric bipolar) membrane based on it. Due to its chelating properties, the phosphoric acid ionogenic group can be highly

effective in altering the specific selectivity for certain metal cations (primarily rare earth and d elements).

The authors successfully developed a method for producing thin films from sulfonated polytetrafluoroethylene (SPTFE). The films were obtained by pouring a specified amount of ionomer solution onto the surface of the substrate membrane (for producing bilayer membranes) or directly onto a glass plate (for producing individual films). Bulk-modified membranes can be produced by adding phosphorylated Boltorn H20 to a solution of sulfonated polytetrafluoroethylene, followed by casting the mixture onto a glass plate. The properties of the resulting bulk-modified SPTFE membrane can be regulated by changing the amount of P-H20 in the mixture.

The objective of this study is to determine the influence of the quantity of introduced P-H20 into the matrix of sulfonated polytetrafluoroethylene on the physicochemical and electrochemical properties of the resulting SPTFE film produced via ionomer solution casting, as well as on the ion transport process through such membranes.

## 2. Materials and Methods

In the conducted study, the following chemicals were used: isopropyl alcohol, 99.9%, CAS-No 67-63-0; sodium chloride 99.9%, CAS-No 7647-14; calcium chloride, CAS-No. 10043-52-4; and nitric acid with a standard titer, CAS-No. 7697-37-2. All reagents were manufactured by JSC "VEKTON," Russia.

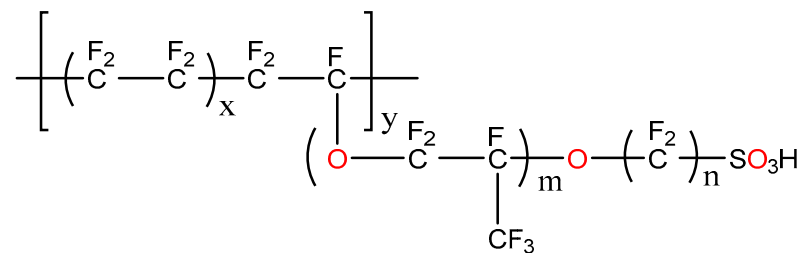
The synthesis of phosphorylated hyperbranched polymer was based on the Boltorn H20 hyperbranched polymer with 16 hydroxyl end groups per molecule, from Polymer Factory Sweden AB (<https://www.polymerfactory.com/product-page/boltorn-premium-h20>) (accessed on 5 December 2023)), Switzerland. The product's purity was 99.9%.

To produce membrane films (SPTFE), a solution of perfluorinated sulfonated polymer in isopropyl alcohol at a 10% mass concentration was used, produced by JSC "Plastpolimer," St. Petersburg, Russia.

### 2.1. SPTFE Membrane

The membranes under investigation were obtained using the casting method, by pouring a polymer solution onto a specially prepared form made of inorganic glass. The polymer solution was poured at room temperature ( $25 \pm 2$  °C) and left to stand for 24 h until completely dry.

The sulfonated perfluoroethylene membranes are basically the same in polymeric structure as the Russian MF-4SK membrane. The latter is a Russian analogue of the Nafion membrane. MF-4SK and Nafion are derived from copolymers of tetrafluoroethylene and perfluorovinyl ether that terminate in a sulfonic acid group (Scheme 1). The Nafion membrane, specifically, is a random copolymer with an electrically neutral semicrystalline polymer backbone (polytetrafluoroethylene) and randomly tethered side-chains with pendant ionic groups (polysulfonyl fluoride vinyl ether) associated with specific counterions (e.g.,  $\text{SO}_3^- + \text{H}^+ \rightarrow \text{SO}_3\text{H}$ ).



**Scheme 1.** Structural unit of the Nafion membrane.

These membranes exhibit natural phase separation due to the dissimilar nature of the covalently bonded pendant groups and the backbone, which is further enhanced by

solvation (introduction of water or solvent molecules). The microphase separation is a key structural feature, involving clustering of ionomer groups.

The Gierke's cluster-channel model, based on X-ray diffraction studies, provides a fundamental model for the structure of the Nafion membrane [27]. According to this theory, the sulfonic-acid side chains in Nafion are organized in clusters of approximately 4 nm. The transfer of  $H^+$  protons occurs through narrow, water-filled channels by means of the sulfonic-acid-terminated side chains (Figure 1).

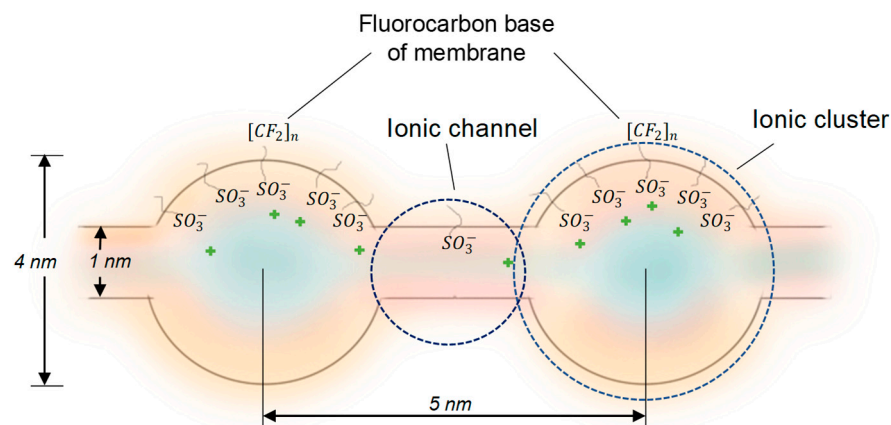
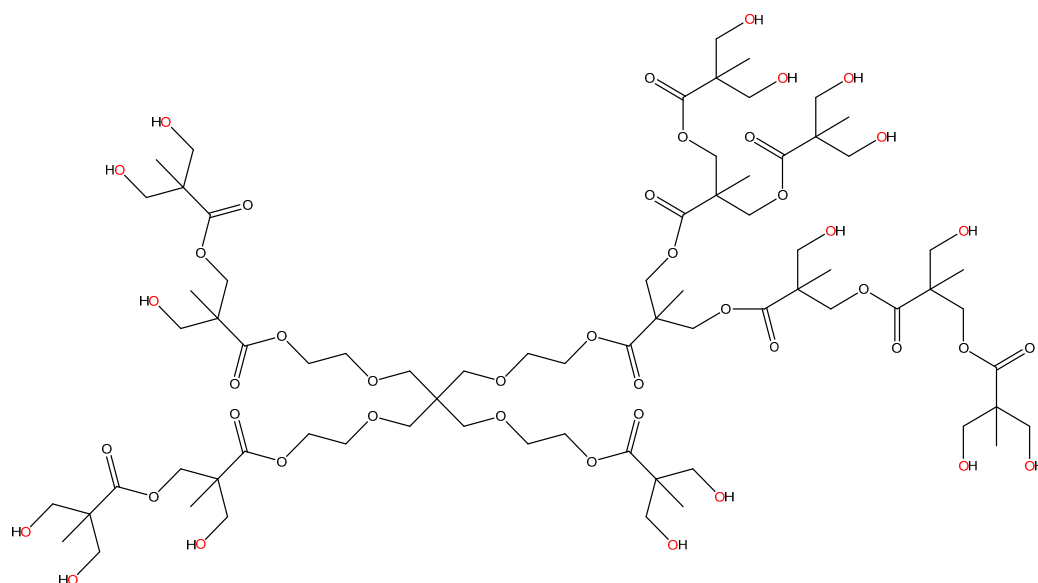


**Figure 1.** Gierke cluster-channel model of a swollen Nafion-type membrane.

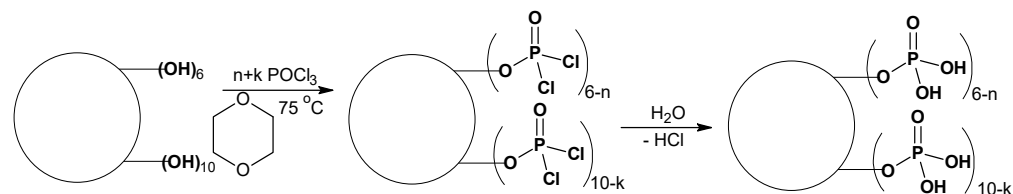
## 2.2. P-H2O Synthesis

The chemical structure of the asymmetric hyperbranched polymer Boltorn H20 is shown in Scheme 2 [28].



**Scheme 2.** The chemical structure of Boltorn H20 [28] with 16 OH groups.

The solution of Boltorn H20 (4.37 g, 40.0 mmol hydroxyl groups) in dioxane was treated with stoichiometric amounts of  $POCl_3$  (3.75 mL, 40.0 mmol). The reaction mixture was heated to 75 °C for 1 h with triethylamine as the catalyst, yielding phosphorylated polyether. The reaction mixture was then treated with distilled water, and the resulting product was precipitated from the solution and dried in a vacuum desiccator. Scheme 3 illustrates the phosphorylation process of Boltorn H20 using  $POCl_3$ .



**Scheme 3.** Scheme of phosphorylation of the asymmetric hyperbranched polymer Boltorn H20.

The presence of phosphoric acid groups in the polymer molecule was confirmed using IR and NMR spectroscopy. In the IR spectrum of the phosphorylated product, a distinctive intense band appears at  $1002\text{ cm}^{-1}$ , corresponding to P-O-C bond vibrations. Additionally, broad and intense bands in the  $2700\text{--}2500\text{ cm}^{-1}$  range indicate vibrations of P-O-H groups, while a decrease in absorption intensity in the  $3500\text{--}3200\text{ cm}^{-1}$  range signifies a reduction in the number of terminal hydroxyl groups. In the  $^{31}\text{P}$  NMR spectrum of phosphorylated Boltorn H20, three broad signals are observed in the range of 6.6 to  $\approx 0.5$  ppm. The presence of three signals is attributed to the existence of phosphate groups linked to varying numbers of alkyl radicals. This variability arises due to the high reactivity of  $\text{POCl}_3$ , which can interact with one terminal OH group, as well as two or three OH groups.

The obtained phosphorylated hyperbranched polymer was dissolved in isopropyl alcohol to obtain a 20% mass fraction solution. To produce the investigated SPTFE membranes with different phosphorylated dendrimers, a 10% SPTFE solution in isopropanol was mixed with a 20% solution of phosphorylated BOLTORN H20 in different ratios. Complete mixing of the solutions was achieved by immersing the polymer mixture in an ultrasonic bath and keeping it there for 5 h. The membranes were obtained using the casting method. The content of hyperbranched phosphorylated dendrimer in the volume of the membrane varied from 2% to 20% of the dry membrane mass.

### 2.3. Mechanical Properties

The mechanical properties of the experimental membranes were examined at a room temperature of  $25 \pm 2\text{ }^\circ\text{C}$  and a relative humidity of  $20 \pm 2\%$ . Before the measurements, the samples were stored in a desiccator with a constant humidity of 95% for two days. Three strips, each 50 mm long and 10 mm wide, were cut for each type of membrane under investigation. The thickness of each strip was measured using a micrometer immediately before the experiment, taking the average of five points along the entire length of the strip. The distance between the grips of the tensile testing machine was 30 mm, and the stretching speed was 5 mm/min, with a preload of 1 N. The Young's modulus was determined from the slope of the stress-strain curve in the elastic deformation range (2–4%). The yield strength was identified as the point of intersection of the tangents to the elastic and plastic deformation sections. The values of Young's modulus, yield strength, stress, and strain at rupture were obtained for each sample of the tested membranes. The average values for each set of samples were computed, and the measurement error was gauged as the standardized deviation within the sample.

### 2.4. Ion-Exchange Capacity and Water Uptake

The ion-exchange capacity is a critical characteristic of ion-exchange membranes that quantifies the amount of ion-conducting functional groups per gram of the membrane. This property directly influences factors such as ion conductivity, swelling ratio, water uptake, and water/gas permeance. The total capacity can be expressed as mol-eq/mL (volumetric) or mol-eq/gm (based on weight).

The total ion-exchange capacity values of membranes were determined using standard back-titration methods. The cation exchange membrane's total ion-exchange capacity was determined by immersing the membrane in  $\text{H}^+$  ionic form in NaOH solution for 24 hours to fully neutralize the  $\text{H}^+$  ions in the membrane. The unreacted NaOH was titrated by a standardized HCl solution.

The total ion-exchange capacity (*totIEC*) values were calculated as follows:

$$\text{totIEC} = \frac{V_{\text{NaOH}}C_{\text{NaOH}} - V_{\text{HCl}}C_{\text{HCl}}}{m_{\text{wet}}}, \quad (1)$$

where  $V_{\text{HCl}}$  and  $C_{\text{HCl}}$  are the volume and concentration of the standardized HCl solution;  $V_{\text{NaOH}}$  and  $C_{\text{NaOH}}$  are the volume and concentration of the standardized NaOH solution; and  $m_{\text{wet}}$  is the weight of dry or wet membrane.

The water content of ion-exchange membranes is a factor that influences their performance by governing their mechanical rigidity, ionic conductivity, and degradation rates. The drying method is commonly employed to measure water content [29].

$$W = \frac{m_h - m_d}{m_d} \cdot 100\%, \quad (2)$$

is the water content of the membrane, where  $m_d$  and  $m_h$  denote the mass of the dry membrane and the mass of the same membrane after hydration, respectively.

### 2.5. Conductivity and Diffusion Permeability Measurement

Standardized methods were used to determine the diffusion permeability coefficient and specific conductivity measurements [30–32], with all experiments conducted at a constant temperature of 25 °C and repeated at least 3 times.

In the framework of the microheterogeneous model [33], the membrane can be presented as two separate conducting phases: the gel phase and electroneutral solution (intergel). The gel phase (with volume fraction  $f_1$ ) comprises the polymer matrix of the ion exchanger, condensed ion pairs, counterion-fixed group, solution inside the electric double layer, reinforcing fabric, and inert binder. The intergel phase (with volume fraction  $f_2$ ) consists of a solution that mainly fills the macro- and partially mesopores in the ion-exchange membrane phase. In the case of Nafion-type membrane, the electroneutral solution fills central parts of clusters. It is generally accepted that the physicochemical properties of such a solution do not differ from the properties of an equilibrium external solution.

Heterogeneity of membrane structure significantly influences the characteristics of ion exchange membranes. Homogeneous membranes are characterized by a very low electroneutral solution fraction ( $f_2 = 0.02$ – $0.1$ ), lacking macropores and cavities. Conversely, for heterogeneous membranes, this value is notably higher ( $f_2 = 0.2$ – $0.3$ ) owing to the presence of cavities and caverns between different particles.

### 2.6. Current–Voltage Curves and Specific Permselectivity Measurement

The current–voltage characteristics and effective transport numbers of ions through the membrane ( $T_j$ ) were studied using the method of a rotating membrane disk [34]. The application of this method for electromembrane systems is described in detail in several works [35,36]. Schematic depiction of the ion fluxes through the membrane and distribution of electrolyte concentration and density in a device with a rotating membrane disk are shown in Figure 2.

The voltammetric characteristics of the membranes were recorded in a galvanostatic mode, with a stepwise increase in current density. The membrane disk was rotated at a speed of 100 rpm. The solution was fed into the cathode chamber at a rate of  $7.5 \pm 0.1$  mL/min. The initial solution used was either 0.03 M NaCl or a mixed solution of 0.015 M NaCl and 0.0075 M CaCl<sub>2</sub>. The concentrations of electrolytes were chosen in such a manner to make data comparable with our previous findings in [37,38]. The variations in the concentrations of Ca<sup>2+</sup> and Na<sup>+</sup> ions were analyzed using an Aquilon Stayer ion chromatograph.

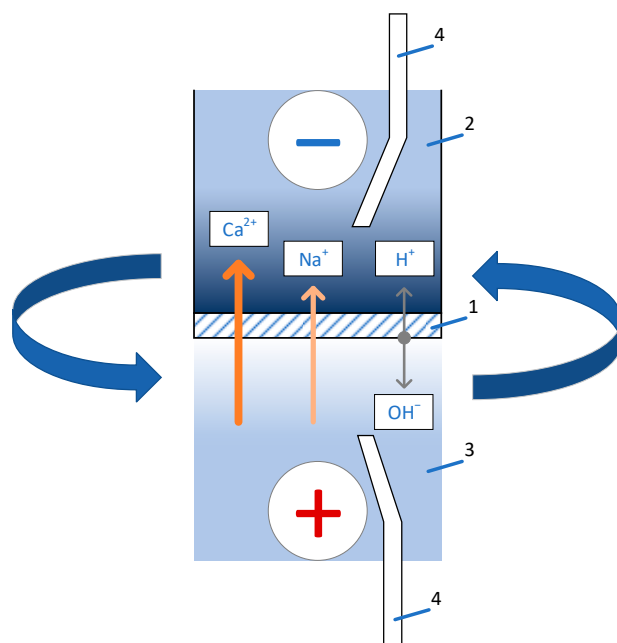


**Figure 2.** Scheme of ion fluxes through the membrane and distribution of electrolyte concentration and density in a device with a rotating membrane disk. 1—Studied membrane, 2—cathode chamber, 3—anode chamber, 4—Luggin capillaries.

The effective transport numbers ( $T_j$ ) were calculated using the following equation:

$$T_j = \frac{\Delta c_j V F}{I t}. \quad (3)$$

Based on the dependences of the effective transport numbers of  $\text{Ca}^{2+}$  and  $\text{Na}^+$  ions on the current density ( $T_j(i)$ ), the permselectivity coefficients ( $P_{1,2}(i)$ ) were calculated using Equation (4):

$$P_{1,2} = \frac{T_1 z_2 c_2}{T_2 z_1 c_1}. \quad (4)$$

### Current–Voltage Curves of Bipolar Membranes

The voltammetric characteristics of bipolar membranes were measured in a four-compartment electrochemical cell. A detailed description of the cell is provided in the work [19]. A dynamic approach was employed to measure the current–voltage characteristics. The test membranes underwent a pre-conditioning period of 30–40 min in an electrochemical cell, where solutions circulated and no current was applied. Subsequently, a Potentiostat/Galvanostat/EIS Analyzer Elins P-45X was utilized to apply a linearly increasing current to the cell, and the resulting current–voltage characteristic was recorded.

The current sweep rate was set at  $2 \cdot 10^{-5}$  A/s.

The current–voltage characteristics of bipolar membranes were measured in 0.5 M NaCl.

## 3. Results and Discussion

### 3.1. Dopant Distribution, Mechanical and Physicochemical Properties

The casting technique used to apply a mixture of two ion polymers offers a distinct advantage in creating materials with a uniformly distributed modifier, as compared to known methods such as sequential diffusion or in situ synthesis in commercial membranes [39,40]. In the latter case, a high concentration of modifier particles is observed on the surface or in a thin layer near the membrane surface, which decreases away from the surface.

The SEM images shown in Figure 3 present the surface of a polytetrafluoroethylene membrane obtained using the casting method, as well as a membrane with a 20% (by

volume) P-H2O content. Void spaces on the surface ranging in size from units to tens of micrometers are clearly visible. Presumably, the phosphorylated dendrimer was located within these cavities; however, during the sample preparation for analysis (vacuuming the electron microscope chamber), the P-H2O not bound to the membrane matrix evaporated. This assumption is also supported by the visible absence of phosphorus in the spectra of local X-ray microanalysis conducted for several areas of the surface. It is worth noting that the sulfur signal (ionogenic groups within the sulfonated polytetrafluoroethylene) is insignificant in these areas compared to the signals of fluorine and carbon. Similar voids are observed in the images of the surfaces of membranes with lower modifier content (Figure 3). Furthermore, with decreasing volume fraction of the modifier, the quantity of such areas on the membrane surface also decreases. A similar formation can also be observed on the cross-section image of the membrane containing 20% P-H2O, indicating that the modifier is uniformly distributed throughout the membrane volume, forming micelles through the formation of hydrogen bonds between dendrimer molecules [41].

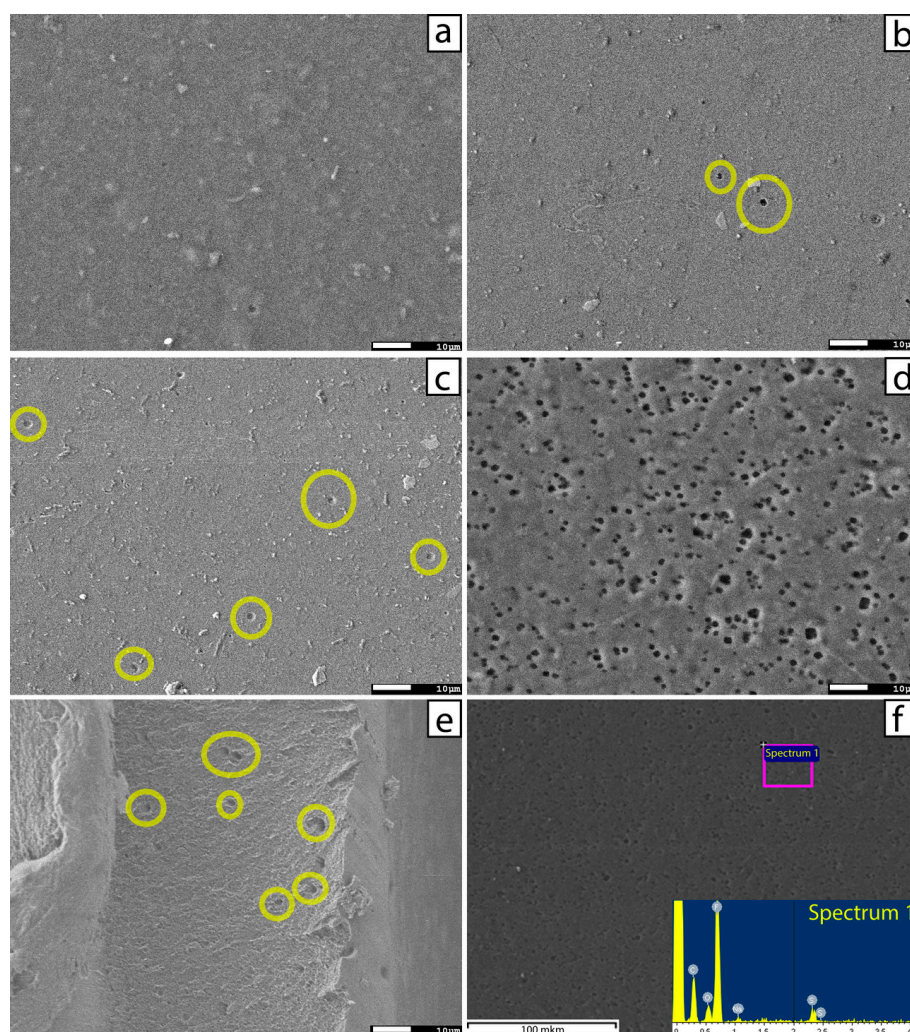


**Figure 3.** SEM images of the surfaces of the pristine SPTFE membrane (a) and membranes containing P-H2O (b–d). The fragment (e) shows the cross-section of the membrane containing 20% P-H2O. The fragment (f) shows results of the elemental analysis of the surface of the membrane containing 20% P-H2O. The volume contents of P-H2O are (b) 5%, (c) 10%, and (d) 20%. Magnification 1000×.

Despite the impossibility of direct confirmation of the presence of P-H2O in the matrix of the cation exchanger, a number of physicochemical characteristics, in addition to the formation of cavities on the surface, indirectly confirm its presence.

The first of these characteristics is the mechanical strength of the obtained samples (Figure 4), and the numerical values of the mechanical parameters are given in Table 1.

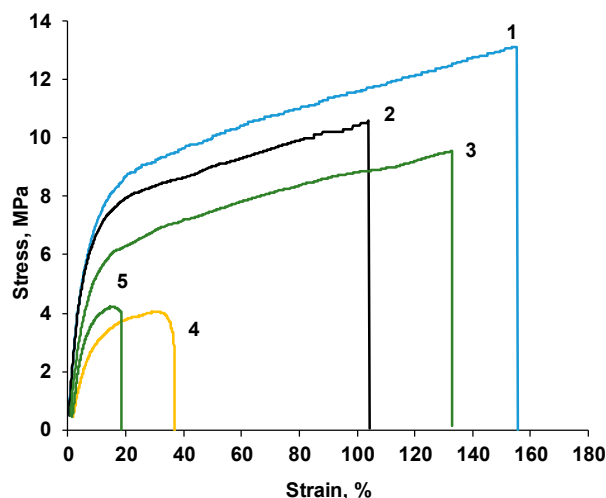


**Figure 4.** The stress–strain curves for the studied membranes. P-H2O volume fractions: 1—0%, 2—2%, 3—5%, 4—10%, and 5—20%.

**Table 1.** Mechanical properties of studied membranes.

| P-H2O Content | Stress, MPa | Strain at Rupture, % | Young's Modulus, MPa | Yield Strength, MPa |
|---------------|-------------|----------------------|----------------------|---------------------|
| 0%            | 12.0 ± 1.1  | 118 ± 44             | 159 ± 12             | 8.0 ± 0.3           |
| 2%            | 10.4 ± 0.7  | 112 ± 7              | 142 ± 8              | 7.2 ± 0.3           |
| 5%            | 11.0 ± 1.3  | 138 ± 10             | 116 ± 8              | 6.5 ± 0.6           |
| 10%           | 3.4 ± 1.4   | 22 ± 9               | 52 ± 22              | 2.8 ± 1.1           |
| 20%           | 5.3 ± 1.0   | 23 ± 12              | 110 ± 31             | 3.7 ± 0.7           |

The mechanical strength and Young's modulus of the obtained membranes decrease with increasing volume fraction of P-H2O. With a P-H2O content of over 30%, it is not possible to obtain mechanically stable films. Such mixtures, after solvent evaporation, resembled a honey-like substance, which is easily disintegrated under external influence.

The reduction in mechanical properties can be explained by two mechanisms of modifier particle localization. In the first case, particles are localized in the hydrophilic cluster area (Figure 5). If the size of the modifier particles is smaller or comparable to the size of the clusters, then, considering the non-sewn nature of the SPTFE matrix, it is possible to increase not only the cluster size, but also the ionic channels connecting individual clusters. This explanation is often encountered within the framework of the pseudo-elasticity model of pores in Nafion-type membranes proposed in the work [42]. In the second case, large modifier particles localize in the area of the hydrophobic perfluorocarbon matrix (backbone). In this case, the forming P-H2O micelles can reach significant sizes of several micrometers, as clearly seen in the SEM results. The formation of microscale areas unbound to both the sulfonated polytetrafluoroethylene material and to each other leads to a substantial reduction in the strength of the resulting membrane, which explains the data presented in the Table 1 for membranes with P-H2O contents of 10%. When these modifier particles are localized, the cluster-channel structure of the SPTFE membrane may also change, for example, through the “contraction” of clusters by the macro particles of the modifier or the rupture of the conducting channel network of the hydrophobic part of the membrane. When the amount of modifier is increased to 20%, the particles may form a separate conducting phase, like a 3D web inside the SPTFE membrane. Then, the mechanical properties of the membrane are somewhat better compared to 10% P-H2O due to the higher stability of this interconnected structure compared with large, but singular, particles.

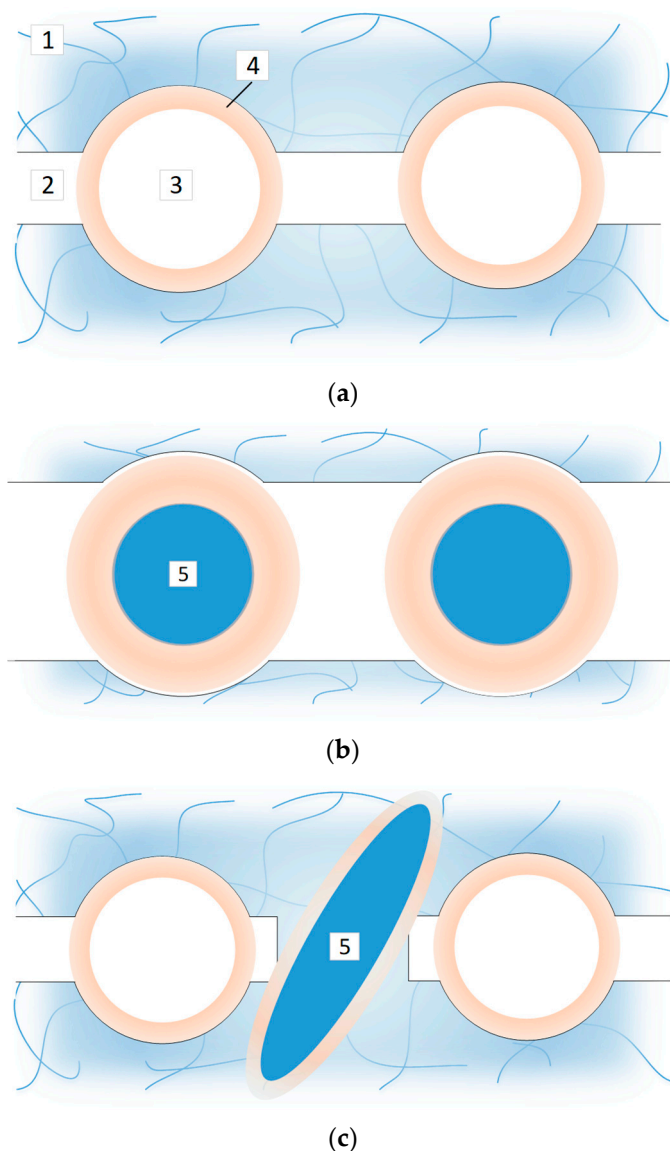


**Figure 5.** Drawing showing changes in the transport-channel structure of the modified membranes: (a) initial transport-channel structure, (b) 2–5% P-H2O content, (c) 10–20% P-H2O content. 1—hydrophobic backbone, 2—ionic channel, 3—ionic ionic cluster, 4—electric double layer, 5—P-H2O particle.

From the results of the measurement of mechanical strength and examination of SEM membrane cross-section images, it can be inferred that the first type of P-H2O incorporation into the SPTFE matrix is characteristic of low modifier quantities (2–5%), while the second type is more characteristic of membranes with a volume fraction of 10–20% of P-H2O.

The results of the measurement of other physicochemical characteristics (ion-exchange capacity, water content, gel phase conductivity, electroneutral solution fraction, integral coefficient of diffusion permeability) are provided in Table 2.

The table indicates a monotonic change in properties with the increase in the modifier quantity in the SPTFE membrane: ion-exchange capacity, water content, and gel phase conductivity decrease, while the electroneutral solution fraction and diffusion permeability increase.

The most likely reason for the decrease in the ion-exchange capacity is the change in the sample density with the increase in the volume fraction of the modifier.

**Table 2.** Physicochemical properties of pristine and modified membranes.

| Volume Fraction of P-H2O, %  | 0           | 2           | 5           | 10          | 20          |
|--|-------------|-------------|-------------|-------------|-------------|
| Ion-exchange capacity, mmol/g <sub>wet</sub>   | 0.83 ± 0.05 | 0.81 ± 0.05 | 0.79 ± 0.05 | 0.72 ± 0.05 | 0.66 ± 0.05 |
| Water uptake, %  | 15.6 ± 0.3  | 15.4 ± 0.3  | 14.7 ± 0.3  | 12.5 ± 0.3  | 10.3 ± 0.3  |
| Gel conductivity, $k_{iso}$ , mS/cm  | 9.7         | 5.3         | 4.2         | 3.7         | 2.8         |
| Intergel fraction, $f_2$   | 0.02        | 0.06        | 0.07        | 0.07        | 0.07        |
| Integral diffusion permeability in 1 M NaCl, $P_m$ , 10 <sup>6</sup> ·cm <sup>2</sup> /s | 0.1 ± 0.05  | 0.3 ± 0.1   | 0.5 ± 0.1   | 0.8 ± 0.1   | 1.0 ± 0.1   |

The reduction in water content may be linked to the removal of some free water from the region of hydrophilic clusters by the modifier particles. For small modifier quantities, the reduction, although following the overall trend, is within the statistical error of the experiment. For membranes with a higher modifier content, the change in water content is more significant and may be associated with the fact that large modifier aggregates occupy a significant portion of the membrane volume and their localization (at least partial) in the hydrophobic part of the membrane may result in reduced hydration compared to the clusters of sulfogroups in the SPTFE membrane.

The decrease in the gel phase conductivity may also be associated with the disruption of the transport channel structure of the membrane. In the case of membranes containing 2 and 5% modifier, partial ion transport blockage may occur within the membrane clusters due to the overlap of the double electrical layers of the cluster walls and modifier particles (Figure 5a). For membranes containing 10% or more modifier, the rupture of the continuous transport channel structure of the membrane may occur (Figure 5b). Interestingly, the decrease in conductivity coincides with an increase in the electroneutral solution fraction and a significant (practically by an order of magnitude) increase in the membrane's diffusion permeability. Typically, an increase in the electroneutral solution fraction leads to an increase in the membrane's conductivity, especially in concentrated solutions. Since the conductivity of the membrane is mainly determined by the counterions and the diffusion permeability by co-ions, such a relationship may indicate that a large number of pathways for co-ion transport are formed in the membrane, with the areas of localization of large modifier particles observed in the SEM results (Figure 3). Substance transport in this case occurs through a mixed mechanism—alternation of the gel phase and electroneutral solution. An unusual mobility–conductivity relationship for Li<sup>+</sup> ions in the perfluorinated matrix was noted in the study [43]. In the study, it was found that samples of perfluoropolyether electrolytes with high diffusivities sometimes exhibited low conductivity. The authors introduced a nondimensional parameter ( $\beta$ ), which accounts for both microscopic diffusivities and conductivity, revealing that  $\beta$  is sensitive to the end-group chemistry. For ethoxylated electrolytes, the parameter approaches unity—the expected value for electrolytes adhering to the Nernst–Einstein equation. Conversely, perfluoropolyether electrolytes lacking ethoxy groups show parameter values significantly lower than one, suggesting a considerable discrepancy between microscopic and continuum transport numbers for Li<sup>+</sup>, potentially due to the electrostatic coupling of the cation and anions (fixed groups).

### 3.2. Current–Voltage Curves and Mechanisms of Ion Transport

The current–voltage curves of ion exchange membranes are typically divided into three regions: the underlimiting current region (also known as the ohmic region or linear region), the limiting current plateau, and the overlimiting current region.

In underlimiting current regimes, it is conventionally assumed that ion transport is purely electrodiffusive, and the ion flux through the membrane linearly depends on the current density. However, recent studies have noted that, in addition to electrodiffusion, underlimiting current regimes may exhibit effects of equilibrium electroconvection [44–46], characterized by an excess of the experimentally determined limiting current in an electromembrane system over the theoretically calculated value. This ion transport is associated with the electroosmosis of the first kind (as per the classification of Dukhin–Mishchuk [47])

and is not electrodiffusive. The ability of ion exchange membranes to exhibit equilibrium electroconvection is determined by the magnitude and sign of the surface charge, its hydrophobicity, and the presence of geometric or electrical heterogeneities [48–50].

The limiting current plateau corresponds to a state where the concentration of charge carriers (ions) at the interface of the depleted diffusion layer/membrane decreases to very low levels, approaching zero. The appearance of a sufficiently thin layer in which mobile charge carriers are effectively absent leads to an increase in the potential drop in the system with practically no increase in current. Analogous to classic electrode systems, this state is referred to as the limiting current. In contrast to electrode systems, in electromembrane systems, the growth of the potential drop at the interface of the depleted diffusion layer/membrane leads to the appearance of conjugated effects of concentration polarization. Two main phenomena that arise with the increase in the potential drop are the water-splitting [51,52] and non-equilibrium electroconvection (electroosmosis of the second kind according to the Dukhin–Mishchuk classification [53]). These phenomena lead to the appearance of charge carriers at the membrane surface and to the deviation of the current–voltage curve from the linearity of the limiting current plateau, transitioning the system into an overlimiting current mode.

Depending on the chemical nature of the ion exchange membrane, the primary mechanism of ion transport in the overlimiting state may be either electroconvection [54,55] or a process known as “water splitting” [10,52,56]. There are also studies demonstrating the potential transition from one mechanism to the other [57]. Typically, water splitting is considered an undesirable process because, firstly, it alters the pH in the pre-membrane space, and secondly, the transport of hydrogen and hydroxide ions does not significantly increase the ion transport of salt (except for a slight increase in useful mass transfer due to the exaltation effect [58]). Occasionally, this effect can be utilized to involve initially electroneutral particles in mass transfer through protonation/deprotonation reactions [59]. On the other hand, the development of electroconvection is seen as a positive process because it allows for an increase in the salt ion flux beyond the limiting value [54,55]. However, the applicability of this phenomenon is limited by the fact that the required potential drop (and consequently, the energy consumption) often far exceeds the increase in the ion flux.

The current–voltage characteristics of the SPTFE membrane and a modified membrane containing 10% P-H2O in a 0.03 M NaCl solution are presented in Figure 6.

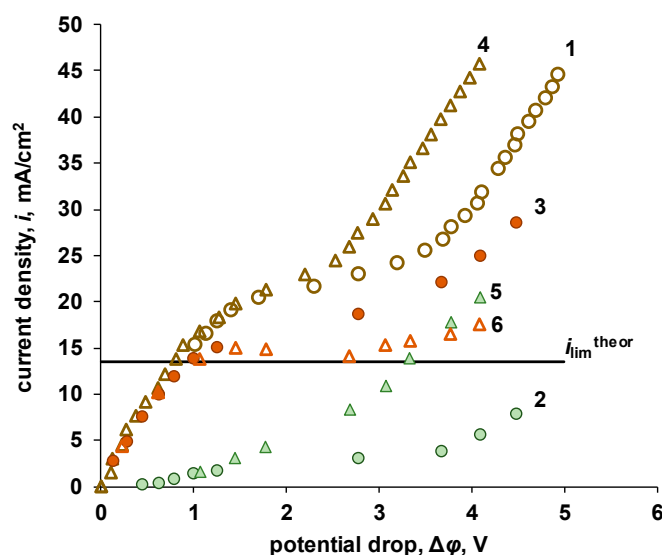


**Figure 6.** Current–voltage curves for pristine SPTFE membrane and membrane with 10% P-H2O obtained in 0.03 M NaCl. 1—total CVC for SPTFE, 2—water-splitting product current for SPTFE, 3—salt current corrected for exaltation effect for SPTFE, 4—total CVC for 10% P-H2O, 5—water-splitting product current for 10% P-H2O, 6—salt current corrected for exaltation effect for 10% P-H2O,  $i_{\text{lim}}^{\text{theor}}$ —theoretical value of the limiting current density.

The current–voltage curves presented in the figure show that volumetric modification does not have a significant impact on the magnitude of the limiting current in the electromembrane system. The original membrane exhibits a limiting current of 18 mA/cm<sup>2</sup>, while the modified membrane shows a limiting current of 17 mA/cm<sup>2</sup>. In both cases, the experimentally determined limiting current exceeds the value theoretically calculated using the Pierce equation. This particular peculiarity of membranes made of sulfonated polytetrafluoroethylene has been previously reported in [60–62]. The theoretical value of the limiting current for the studied system is 13.5 mA/cm<sup>2</sup>.

The modified membrane has a smaller limiting current plateau and enters the overlimiting state earlier. However, the ion transport mechanism in the overlimiting state differs for the investigated membranes. For the SPTFE membrane, the contribution of water splitting is lower compared to the modified membrane, while the fraction of current carried by salt ions is higher. This indicates that electroconvection is the primary ion transport mechanism in the overlimiting state for the SPTFE membrane. In contrast, the modified membrane exhibits a significant contribution of water splitting to the overall mass transfer, and the salt ion flux, even taking the exaltation effect into account, is lower compared to the SPTFE membrane.

The increase in the contribution of water splitting to the overall mass transfer in the modified membrane can be explained by the presence of modifier particles on the membrane surface. The phosphoric acid groups contained in these particles are among the most active catalysts for the water-splitting reaction, as indicated by the range of catalytic activity of ionogenic groups [52].

Zabolotskiy et al. [46] proposed a methodology to assess the contributions of different mechanisms to the overall mass transfer in an electromembrane system. Assuming that in the underlimiting current regime, ion transport occurs either solely through electrodiffusion or through both electrodiffusion and equilibrium electroconvection, the contribution of the latter to the limiting current can be found to be the difference between the experimental limiting current and the theoretical value calculated using the Pierce equation:

$$\beta_{\text{eq}} = \frac{i_{\text{lim}}^{\text{exp}} - i_{\text{lim}}^{\text{theor}}}{i_{\text{lim}}^{\text{exp}}}. \quad (5)$$

In the limiting and overlimiting states, the contribution of non-equilibrium electroconvection can be assessed, taking into account the partial current of water-splitting products and the exaltation current:

$$\beta_{\text{n-eq}} = \frac{i - i_{\text{lim}}^{\text{exp}} - i_w - i_{\text{exz}}}{i}. \quad (6)$$

The exaltation current was assessed using the Kharkats equation [58]:

$$i_{\text{exz}} = \frac{D_+}{D_{\text{OH}^-}} i_w. \quad (7)$$

The total current of salt ions in the overlimiting current mode consists of the experimental limiting current, the exaltation current, and the current resulting from electroconvection.

$$i_s = i - i_w. \quad (8)$$

Using Equation (5), it was found, that the equilibrium electroconvection contributes 25% to the overall mass transfer in the system with the SPTFE membrane. For the modified membrane containing 10% P-H2O, the contribution of electroconvection is 20%. The slight observed difference in the contributions of equilibrium electroconvection corresponds to the observed difference in the magnitudes of the limiting currents (18 and 17 mA/cm<sup>2</sup>). It can be concluded that the presence of P-H2O particles on the surface of the SPTFE membrane slightly reduces its ability to develop equilibrium electroconvection, leading

to a decrease in the magnitude of the limiting current in the electromembrane system. This phenomenon may be due to a decrease in the hydrophobicity of the SPTFE surface caused by the appearance of P-H2O particles. We hypothesize that P-H2O particles should have sufficiently low hydrophobicity, given that the micelles formed by the molecules of phosphorylated Boltorn H20 contain hydroxyl and phosphonate groups capable of forming hydrogen bonds with water molecules. The observed effect is contrary to the effect shown in work [63], where the application of a hydrophobic non-conductive modifier to the membrane surface led to the development of equilibrium electroconvection and an increase in the limiting current.

Bulk modification also alters the overlimiting current transfer. An assessment of the contribution of various mechanisms to the overall mass transfer in the electromembrane system at fixed potential drops is presented in the Table 3 for a pristine membrane and SPTFE membrane with 10% of P-H2O.

**Table 3.** Contribution of different transport mechanisms to the overall mass transfer at different potential drops in the studied system.

| Potential Drop               | Membrane  | SPTFE | SPTFE+10% P-H2O |
|------------------------------|---|-------|-----------------|
|                              | Volume fraction of P-H20, %                                   | 0     | 10              |
|                              | Limiting current density, mA/cm <sup>2</sup>                  | 18    | 17              |
| $\Delta\varphi = 1\text{ V}$ | Total current, mA/cm <sup>2</sup>                             | 14.8  | 16.4            |
|                              | Salt ion current, mA/cm <sup>2</sup>                          | 13.6  | 14.6            |
|                              | Water-splitting product current, mA/cm <sup>2</sup>           | 1.3   | 1.8             |
|                              | Non-equilibrium electroconvection current, mA/cm <sup>2</sup> | -     | -               |
|                              | Exaltation current, mA/cm <sup>2</sup>                        | 0.2   | 0.3             |
| $\Delta\varphi = 2\text{ V}$ | Total current, mA/cm <sup>2</sup>                             | 21.3  | 21.7            |
|                              | Salt ion current, mA/cm <sup>2</sup>                          | 19.1  | 16.9            |
|                              | Water-splitting product current, mA/cm <sup>2</sup>           | 2.2   | 4.9             |
|                              | Non-equilibrium electroconvection current, mA/cm <sup>2</sup> | 1.8   | -               |
|                              | Exaltation current, mA/cm <sup>2</sup>                        | 0.3   | 0.7             |
| $\Delta\varphi = 4\text{ V}$ | Total current, mA/cm <sup>2</sup>                             | 30.4  | 44.5            |
|                              | Salt ion current, mA/cm <sup>2</sup>                          | 25.3  | 24.8            |
|                              | Water-splitting product current, mA/cm <sup>2</sup>           | 5.1   | 19.8            |
|                              | Non-equilibrium electroconvection current, mA/cm <sup>2</sup> | 7.6   | 4.9             |
|                              | Exaltation current, mA/cm <sup>2</sup>                        | 0.7   | 2.8             |

The data shown in the table reveal that the total current on the modified membrane is higher, while the current of salt ions (useful mass transfer) is lower. This difference increases with increasing potential drop. Moreover, for the SPTFE membrane, the contribution of non-equilibrium electroconvection begins to manifest earlier; already at a potential drop of 2 V, it accounts for 8% of the total current. The contribution of exaltation current for the SPTFE membrane is extremely low, not exceeding 5%, attributed to the low current of water-splitting products. Conversely, for the modified membrane, there is an increase in the current carried by H<sup>+</sup>/OH<sup>-</sup> ions. This is due to the high catalytic activity of phosphoric acid groups of the modifier in the water-splitting reaction. As a result of the water-splitting reaction occurring on the surface of the SPTFE+P-H2O membrane, hydroxide ions appear in the solution. These ions “blur” the space-charge region, reduce the electrical field strength, and lead to a decrease in the volumetric electric force. All these factors contribute to a decrease in electroconvective transport at overlimiting currents. While for the SPTFE membrane, the contribution of non-equilibrium electroconvection to overlimiting mass transfer begins to manifest already at a potential drop of 1.5 V, for the modified membrane, it requires a potential drop larger than 3.2 V.

Therefore, when a phosphorylated dendrimer is added to the SPTFE membrane, it reduces the impact of non-equilibrium electroconvection on overlimiting current regimes and enhances the rate of the water-splitting reaction. Meanwhile, there is a minor change

in the magnitude of the limiting current density due to the decreased contribution of equilibrium electroconvection on the modified membrane. This latter phenomenon is likely associated with a modification of the membrane's surface hydrophobicity due to the localization of some proportion of the modifier particles on it.

The current–voltage characteristics of the SPTFE membrane and modified membranes with different bulk contents of the phosphorylated dendrimer obtained in a mixed electrolyte of 0.015 M NaCl + 0.0075 M CaCl<sub>2</sub> are presented in Figure 7.

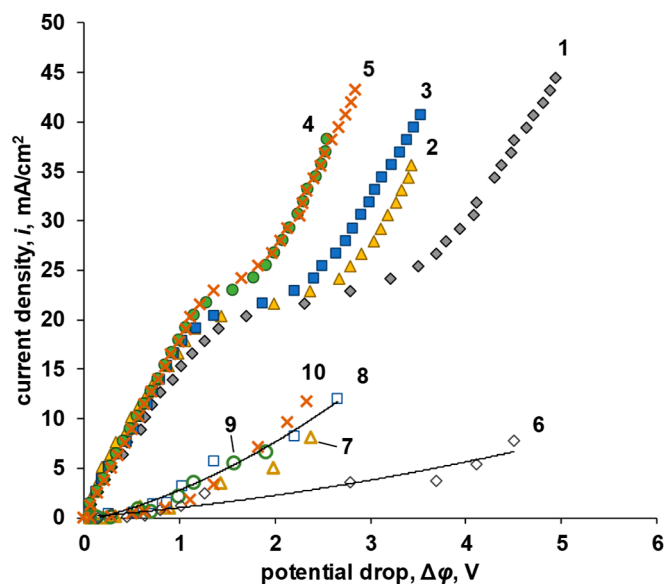


**Figure 7.** Current–voltage curves for a pristine SPTFE membrane and membranes with varying P-H2O contents in a 0.015 M NaCl + 0.0075 M CaCl<sub>2</sub> solution. Curves 1–5 represent the total currents, while curves 6–10 represent the partial currents carried by OH<sup>−</sup> ions. The P-H2O volume fractions are as follows: 0% for curves 1 and 6 (pristine SPTFE membrane), 2% for curves 2 and 7, 5% for curves 3 and 8, 10% for curves 4 and 9, and 20% for curves 5 and 10.

The observed patterns during the investigation of membranes in a sodium chloride solution persist when transitioning to ternary electrolytes containing a mixture of sodium chloride and calcium chloride: the introduction of P-H2O into the SPTFE membrane reduces the length of the limiting current plateau; an increase in the flux of water-splitting products is observed for the modified membranes. However, no correlation with the volumetric fraction of the modifier is observed for the latter. One possible reason for this is that the water-splitting product flux depends on two factors: the electric field strength at the boundary of the depleted diffusion layer/membrane and the concentration of catalytically active groups. With the increase in the volumetric fraction of the modifier, the number of catalytically active centers on the membrane surface increases, while the potential for transitioning to the overlimit state decreases, meaning the intensity of the electric field at a fixed current density decreases. These two effects offset each other.

One should also take into account the possibility of super-equivalent absorption of calcium ions from the solution, discovered in the work [64]. The specific adsorption of Ca<sup>2+</sup> ions leads to a change in the membrane surface charge density from negative to positive. The latter causes a delay in the onset of unstable electroconvection, that is, a reduction in membrane performance.

The contributions of various mechanisms to the overall mass transfer at a fixed potential drop and at a fixed current density are presented in Tables 4 and 5.

**Table 4.** Contributions of different transport mechanisms to the overall mass transfer at a potential drop of 2 V in the studied system.

| Membrane  | SPTFE |      | SPTFE+P-H20 |      |      |
|---|-------|------|-------------|------|------|
| Volume fraction of P-H20, %                                   | 0     | 2    | 5           | 10   | 20   |
| Limiting current density, mA/cm <sup>2</sup>                  | 18    | 18.5 | 19          | 21   | 22   |
| Total current, mA/cm <sup>2</sup>                             | 21.3  | 16.4 | 21.8        | 21.9 | 26.7 |
| Salt ion current, mA/cm <sup>2</sup>                          | 19.1  | 14.6 | 16.1        | 14.3 | 19.2 |
| Water-splitting product current, mA/cm <sup>2</sup>           | 2.2   | 1.8  | 5.7         | 7.6  | 7.5  |
| Non-equilibrium electroconvection current, mA/cm <sup>2</sup> | 1.8   | -    | -           | -    | -    |
| Exaltation current, mA/cm <sup>2</sup>                        | 0.3   | 0.3  | 1.5         | 2.0  | 2.0  |

**Table 5.** Contributions of different transport mechanisms to the overall mass transfer at a constant current density of 25 mA/cm<sup>2</sup> in the studied system.

| Membrane  | SPTFE |      | SPTFE+P-H20 |      |      |
|---|-------|------|-------------|------|------|
| Volume fraction of P-H20, %                                   | 0     | 2    | 5           | 10   | 20   |
| Potential drop, V   | 3.4   | 2.8  | 2.4         | 1.9  | 1.8  |
| Salt ion current, mA/cm <sup>2</sup>                          | 21.5  | 14.8 | 14.3        | 18.7 | 18.6 |
| Water-splitting product current, mA/cm <sup>2</sup>           | 3.4   | 10.6 | 10.1        | 6.8  | 6.6  |
| Non-equilibrium electroconvection current, mA/cm <sup>2</sup> | 2.7   | -    | -           | -    | -    |
| Exaltation current, mA/cm <sup>2</sup>                        | 0.9   | 2.8  | 2.7         | 1.8  | 1.8  |

As can be seen from Table 4, at a fixed potential drop close to or slightly exceeding the potential drop at the limiting current on the modified membranes, the water-splitting reaction actively occurs. Moreover, with the increase in the volumetric fraction of the modifier, the flux of water-splitting products increases. This dependency directly indicates that the quantity of modifier particles on the membrane surface increases with the growth of the volumetric fraction of P-H20. Under these conditions, there is no electroconvection development on the modified membranes, and the useful mass transfer slightly increases due to the exaltation effect.

Interestingly, in the mixed solution containing sodium chloride and calcium chloride, the limiting current slightly increases with the increase in the volumetric fraction of the modifier compared to the original membrane rather than decreasing, as in the case of a solution containing only sodium chloride.

When considering the transport mechanisms in the membranes at a constant current density (Table 5), the following regularities are observed: The introduction of the modifier leads to an almost twofold reduction in the salt ion flux. Meanwhile, as the volumetric fraction of the modifier increases, there is an increase in useful mass transfer and a decrease in the portion of the current carried by water-splitting products. Additionally, the total potential drop in the electromembrane system decreases. Similar to the conditions of a constant potential drop, there is no contribution of non-equilibrium electroconvection to the overall mass transfer on the modified membranes under these conditions.

Under conditions of constant current density, the modified membranes can be divided into two groups. Membranes containing a modifier with a volumetric fraction of less than 10% demonstrate larger potential drops and a greater contribution of the water-splitting reaction to the overall mass transfer. Membranes with a volumetric fraction of P-H20 > 10% show a greater contribution of salt ion transport to the overall mass transfer and smaller potential drops. The high concentration of P-H20 on the membrane's surface may explain this, allowing the water-splitting reaction on such membranes to occur with a smaller potential drop, and additional charge carriers appear earlier.

Thus, under a constant current density, the concentration of modifier particles on the membrane surface plays a more significant role. In contrast, when operating in a potentiostatic mode, the magnitude of the potential drop itself is more crucial. This is

because at equal values of the potential drop, membranes with a higher volumetric fraction of the modifier will more actively participate in the water-splitting reaction.

An important characteristic that can largely determine the feasibility of using specific ion-exchange membranes is the energy consumption for substance transport. From the obtained data, the specific energy consumption can be calculated as follows:

$$E = \frac{i}{i_s} \Delta\varphi F. \quad (9)$$

The first factor essentially represents the effective transport number of all counterions through the membrane. The calculated values of the specific energy consumption at constant current densities of 15 (underlimiting state) and 25 (overlimiting state) mA/cm<sup>2</sup> are shown in Figure 8.

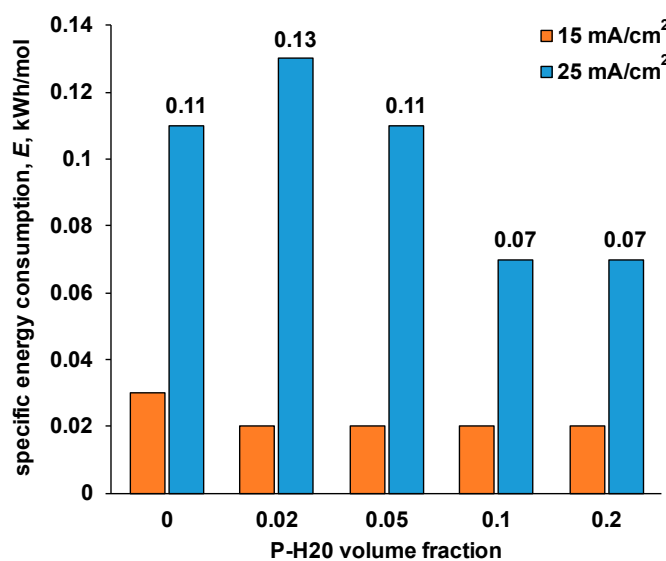


**Figure 8.** Specific energy consumption at different current densities for pristine SPTFE and modified membranes.

At a deliberately underlimiting current density (15 mA/cm<sup>2</sup>), the specific energy consumption for the original membrane is 0.03 kWh/mol, while for all modified membranes, it is 0.02 kWh/mol.

More interesting results are obtained when considering the results obtained at a current density of 25 mA/cm<sup>2</sup> (a slight excess of the limiting current for all the studied membranes). For membranes containing 2% and 5% of the modifier, there is a certain increase in specific energy consumption directly related to the relatively high potential drop and the low effective counterions transport number. In contrast, for modified membranes containing 10% and 20% of the modifier, there is a 40% reduction in energy consumption compared to the SPTFE membrane, despite the overall reduction in salt ion transport. This phenomenon is associated with the reduction in the potential drop in the system.

Thus, these membranes can be used in the electro dialysis process when the processed solution is not highly sensitive to changes in pH.

### 3.3. Prospects for Application

Due to the high activity observed in the water-splitting reaction and the phosphoric acid group's capability to form complexes with multivalent ions, the materials obtained could be utilized for ion separation processes or serve as a catalytic layer or cation-exchange layer in bipolar membranes.

### 3.3.1. Monovalent/Divalent Selectivity

The study of the specific selectivity of the membranes was conducted in a mixed solution containing 0.015 M NaCl and 0.0075 M CaCl<sub>2</sub>. The results of the investigation of the dependence of the Specific permselectivity coefficient on the dimensionless current density are presented in Figure 9.

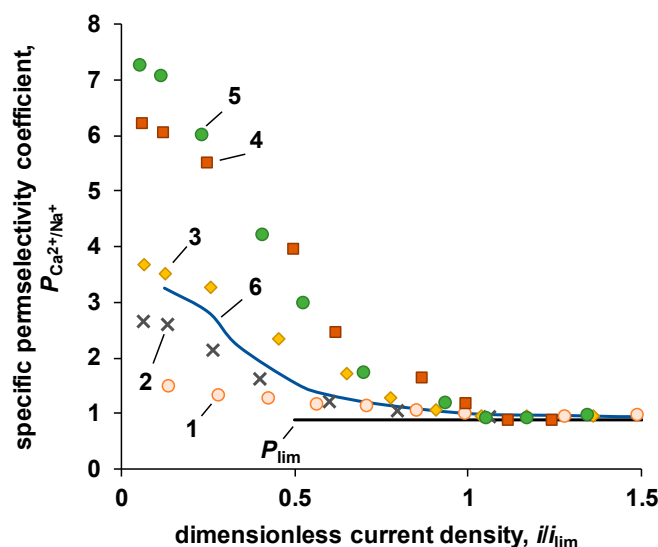


**Figure 9.** Specific permselectivity coefficient between Ca<sup>2+</sup> and Na<sup>+</sup> as a function of dimensionless current density for studied membranes. P-H2O volume fraction: 1—0%, 2—2%, 3—5%, 4—10%, 5—20%, 6—MK-40,  $P_{lim}$ —limiting value of the specific permselectivity coefficient.

As can be seen from the figure, the original SPTFE membrane exhibits weak selectivity towards divalent ions. The introduction of P-H2O with volumetric fractions of 2% and 5% leads to an increase in selectivity towards divalent ions to a level comparable to that of the MK-40 membrane. Introducing a greater amount of the modifier further increases the specific permselectivity. For the membrane with a volumetric fraction of P-H2O at 20%, the maximum value of the specific permselectivity coefficient is 7.2, which is five times higher than the value for the SPTFE membrane, which is 1.5. According to theoretical considerations of the dependence of the specific permselectivity coefficient on the dimensionless current density, as the current approaches the limiting value, the coefficient decreases. At currents close to or exceeding the limit, the specific selectivity of the membrane ceases to depend on the nature of the membrane, but is determined by the charges of the transferred ions and the ratio of their diffusion coefficients [65]. For the Ca<sup>2+</sup>/Na<sup>+</sup> pair, the limiting value of the specific permselectivity coefficient is 0.89. However, for membranes containing 10% and 20% of the modifier, the specific permselectivity coefficient remains sufficiently high (around 4), up to a value of  $i/i_{lim} = 0.5$ .

The high values of the specific permselectivity coefficient, together with the practically unchanged value of the limiting current, enables the use of modified membranes with a volumetric fraction of phosphorylated dendrimer at 10–20% for the separation of single and multivalent ions.

### 3.3.2. Bipolar Membranes

The high catalytic activity of membranes containing phosphorylated Boltorn H20 in the water-splitting reaction suggests that they could be effectively used as the cation-exchange layer of a bipolar membrane. The anion-exchange layer, in turn, could be made of a copolymer of DADMAC and ethyl methacrylate (this material is extensively described in [46]), as previously developed by the authors. The thickness of the anion-exchange layer and the thickness of the cation-exchange layer were 200  $\mu\text{m}$ .

Since the cation-exchange and anion-exchange layers of the bipolar membrane are made of polymers of different natures, the layers were cast using the same solvent—*isopropyl alcohol*—to enhance adhesion between them. This method allows for partial dissolving of the solidified polymer during the application of the cation-exchange layer onto the anion-exchange layer, enabling the intertwining of the chains of the cation-exchange and anion-exchange layers.

For comparison, a bipolar membrane was prepared in which the cation-exchange layer was made of unmodified SPTFE.

The current–voltage characteristics of the obtained bipolar membranes in 0.5 M NaCl are shown in Figure 10.

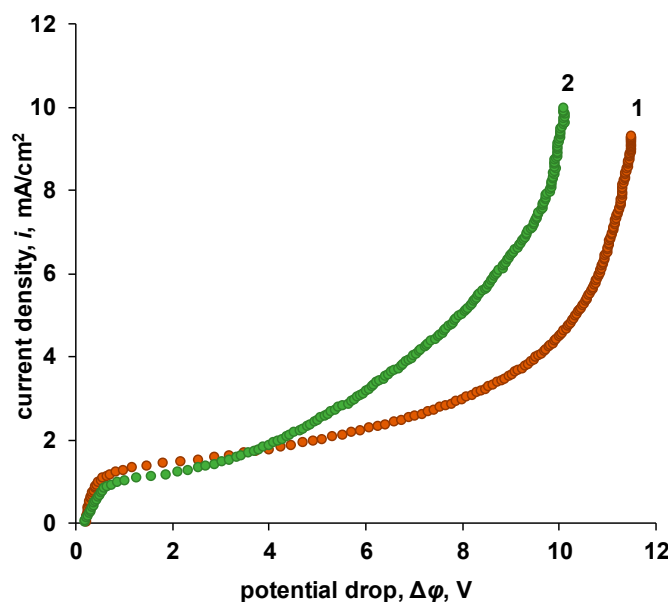


**Figure 10.** Current–voltage curves of homogeneous bipolar membranes: 1—cation-exchange layer is made of SPTFE, 2—cation-exchange layer is made of SPTFE+20% P-H2O.

As seen in the figure, using a membrane modified with P-H2O as the cation-exchange layer of the bipolar membrane allows for a reduction in the operating voltage on the bipolar membrane from 11.3 V to 9.8 V at a current density of 8 mA/cm<sup>2</sup>. However, both obtained membranes have high voltages that preclude their use in real processes.

The high voltage for the homogeneous membrane is due to the low initial activity of the ionogenic groups in the anion-exchange and cation-exchange layers. The results obtained for the membrane with the cation-exchange layer made of SPTFE are comparable to the MB-2 membrane [66]. At the same time, when using the modified membrane, the fraction of phosphorylated dendrimer particles in contact with the anion-exchange layer is insufficient for the effective progression of the water-splitting reaction. Additionally, two other factors play a role. Firstly, during the production of membranes, the interpenetration of polymer chains causes the area of the bipolar interface to “blur,” which typically leads to a reduction in the intensity of the electric field at the cation-exchange/anion-exchange boundary. As a result, the water-splitting process occurs later in such systems than in systems with a “sharp” boundary [67]. Secondly, membranes with a high fraction of P-H2O are characterized by high diffusion permeability. The influx of co-ions (salt ions) to the bipolar boundary also reduces the intensity of the electric field and slows down the water-splitting process.

Therefore, to use modified membranes as the cation-exchange or intermediate catalytic layer in bipolar membranes, it is necessary to refine the method of producing bipolar membranes, as well as increase their catalytic activity and decrease the diffusion permeability.

#### 4. Conclusions

In the present work, cation-exchange membranes made of sulfonated polytetrafluoroethylene and bulk-modified membranes with the phosphorylated dendrimer Boltorn H20 were obtained and characterized using various methods, including mechanical, physicochemical, and electrochemical analyses. Despite the fact that we could not directly detect the presence of phosphorus in the structure of the membrane material using SEM and local X-ray microanalysis, a number of indirect indicators (changes in mechanical properties, changes in activity in the water-splitting reaction, and changes in the electrical conductivity and diffusion permeability) indicate the presence of a modifier in the resulting materials. The fact that the observed changes are caused precisely by the presence of P-H20 is indicated by the acceleration of the water-splitting reaction.

Due to the presence of the phosphoric acid group in the modifier, the obtained membranes exhibit high specific permselectivity for calcium ions and possibly towards other multivalent ions like  $Mg^{2+}$ ,  $Sr^{2+}$ ,  $Ni^{2+}$ ,  $Co^{2+}$ ,  $Mn^{2+}$ , etc. Due to the low solubility of lithium phosphate, one can expect an increased selectivity towards  $Li^+$  ions, which is a subject of further investigation. The developed materials show high selectivity towards multivalent (at least calcium) ions, and at the same time retain the high value of the limiting current density. The latter suggests that the ions flux through such membranes is high and is not affected by a possible strong bonding between phosphonic groups and calcium ions.

The introduction of the modifier into the membrane volume leads to the localization of some of its particles on the membrane surface, which, also due to the presence of phosphoric acid groups, results in a change in the mechanisms of overlimiting mass transfer in the electromembrane system. While for the SPTFE membrane, the dominant mechanism of overlimiting mass transfer is the non-equilibrium electroconvection, for the modified membranes, the primary current carriers in the overlimiting state are the water-splitting reaction products. The water-splitting reaction results in a reduction of the potential drop at which the membrane transitions into the overlimiting state, leading to a decrease in specific energy consumption despite the reduction in the current carried by the counterions.

Despite their high activity in the water-splitting reaction, it has not been possible to apply the modified membranes as a catalytic or cation exchange layer in bipolar membranes to date. The homogeneous bipolar membranes obtained have a high operating voltage, thus preventing their effective use in real processes.

Therefore, the bulk-modified membranes can be effectively applied in the separation processes of mono- and multivalent ions with high specific permselectivity coefficient and high ions fluxes.

**Author Contributions:** Conceptualization, A.A.; methodology, A.A. and D.B.; investigation, A.A.; data curation, A.A., D.B. and E.N.; writing—original draft preparation, E.N. and S.M.; writing—review and editing, S.M.; visualization, E.N.; supervision, S.M.; project administration, A.A. and S.M.; funding acquisition, S.M. All authors have read and agreed to the published version of the manuscript.

**Funding:** The study was supported by a grant from the Russian Science Foundation No. 22-23-00357, <https://rscf.ru/project/22-23-00357/>, accessed on 5 December 2023.

**Institutional Review Board Statement:** Not applicable.

**Informed Consent Statement:** Not applicable.

**Data Availability Statement:** The data presented in this study are available on request from the corresponding author.

**Conflicts of Interest:** The authors declare no conflicts of interest.

#### References

1. Luo, T.; Abdu, S.; Wessling, M. Selectivity of Ion Exchange Membranes: A Review. *J. Membr. Sci.* **2018**, *555*, 429–454. [[CrossRef](#)]
2. Helfferich, F.G. *Ion Exchange*; McGraw Hill Book Company, Inc.: New York, NY, USA, 1962; ISBN 0-486-68784-8.
3. Zhang, Y.; Paepen, S.; Pinoy, L.; Meesschaert, B.; Van Der Bruggen, B. Electrodialysis: Fractionation of Divalent Ions from Monovalent Ions in a Novel Electrodialysis Stack. *Sep. Purif. Technol.* **2012**, *88*, 191–201. [[CrossRef](#)]

4. Galama, A.H.; Daubaras, G.; Burheim, O.S.; Rijnaarts, H.H.M.; Post, J.W. Fractioning Electrodialysis: A Current Induced Ion Exchange Process. *Electrochim. Acta* **2014**, *136*, 257–265. [[CrossRef](#)]
5. Ge, L.; Wu, B.; Li, Q.; Wang, Y.; Yu, D.; Wu, L.; Pan, J.; Miao, J.; Xu, T. Electrodialysis with Nanofiltration Membrane (EDNF) for High-Efficiency Cations Fractionation. *J. Membr. Sci.* **2016**, *498*, 192–200. [[CrossRef](#)]
6. Khoiruddin; Ariono, D.; Subagjo; Wenten, I.G.; Ariono, D.; Gede Wenten, I.; Khoiruddin; Ariono, D.; Subagjo; Wenten, I.G.; et al. Surface Modification of Ion-Exchange Membranes: Methods, Characteristics, and Performance. *J. Appl. Polym. Sci.* **2017**, *134*, 1–13. [[CrossRef](#)]
7. Sata, T. Studies on Anion Exchange Membranes Having Permselectivity for Specific Anions in Electrodialysis—Effect of Hydrophilicity of Anion Exchange Membranes on Permselectivity of Anions. *J. Membr. Sci.* **2000**, *167*, 1–31. [[CrossRef](#)]
8. Sata, T.T.; Sata, T.T.; Yang, W. Studies on Cation-Exchange Membranes Having Permselectivity between Cations in Electrodialysis. *J. Membr. Sci.* **2002**, *206*, 31–60. [[CrossRef](#)]
9. Wang, M.; Gao, C. The State-of-The-Art of the Cation Exchange Membrane Having Monovalent Ion Selectivity—A Patent Review. *Recent Pat. Chem. Eng.* **2011**, *4*, 132–140. [[CrossRef](#)]
10. Ran, J.; Wu, L.; He, Y.; Yang, Z.; Wang, Y.; Jiang, C.; Ge, L.; Bakangura, E.; Xu, T. Ion Exchange Membranes: New Developments and Applications. *J. Membr. Sci.* **2017**, *522*, 267–291. [[CrossRef](#)]
11. Ge, L.; Wu, B.; Yu, D.; Mondal, A.N.; Hou, L.; Afsar, N.U.; Li, Q.; Xu, T.T.; Miao, J.; Xu, T.T. Monovalent Cation Perm-Selective Membranes (MCPMs): New Developments and Perspectives. *Chin. J. Chem. Eng.* **2017**, *25*, 1606–1615. [[CrossRef](#)]
12. Park, H.B.; Kamcev, J.; Robeson, L.M.; Elimelech, M.; Freeman, B.D. Maximizing the Right Stuff: The Trade-off between Membrane Permeability and Selectivity. *Science* **2017**, *356*, 1138–1148. [[CrossRef](#)]
13. Chen, Q.B.; Ren, H.; Tian, Z.; Sun, L.; Wang, J. Conversion and Pre-Concentration of SWRO Reject Brine into High Solubility Liquid Salts (HLSLs) by Using Electrodialysis Metathesis. *Sep. Purif. Technol.* **2019**, *213*, 587–598. [[CrossRef](#)]
14. Shaposhnik, V.A.; Kesore, K. An Early History of Electrodialysis with Permselective Membranes. *J. Membr. Sci.* **1997**, *136*, 35–39. [[CrossRef](#)]
15. Culcasi, A.; Gurreri, L.; Zaffora, A.; Cosenza, A.; Tamburini, A.; Cipollina, A.; Micale, G. Ionic Shortcut Currents via Manifolds in Reverse Electrodialysis Stacks. *Desalination* **2020**, *485*, 114450. [[CrossRef](#)]
16. Bazinet, L.; Ippersiel, D.; Montpetit, D.; Mahdavi, B.; Amiot, J.; Lamarche, F. Effect of Membrane Permselectivity on the Fouling of Cationic Membranes during Skim Milk Electroacidification. *J. Membr. Sci.* **2000**, *174*, 97–110. [[CrossRef](#)]
17. White, N.; Misovich, M.; Alemayehu, E.; Yaroshchuk, A.; Bruening, M.L. Highly Selective Separations of Multivalent and Monovalent Cations in Electrodialysis through Nafion Membranes Coated with Polyelectrolyte Multilayers. *Polymer* **2015**, *103*, 478–485. [[CrossRef](#)]
18. Zhao, Y.; Zhu, J.; Ding, J.; Van der Bruggen, B.; Shen, J.; Gao, C. Electric-Pulse Layer-by-Layer Assembled of Anion Exchange Membrane with Enhanced Monovalent Selectivity. *J. Membr. Sci.* **2018**, *548*, 81–90. [[CrossRef](#)]
19. Melnikov, S.; Bondarev, D.; Nosova, E.; Melnikova, E.; Zabolotskiy, V. Water Splitting and Transport of Ions in Electromembrane System with Bilayer Ion-Exchange Membrane. *Membranes* **2020**, *10*, 346. [[CrossRef](#)]
20. Abdu, S.; Wessling, M.; Martí-Calatayud, M.-C.; Wong, J.E.; García-Gabaldón, M.; Wessling, M. Layer-by-Layer Modification of Cation Exchange Membranes Controls Ion Selectivity and Water Splitting. *ACS Appl. Mater. Interfaces* **2014**, *6*, 1843–1854. [[CrossRef](#)]
21. White, N.; Misovich, M.; Yaroshchuk, A.; Bruening, M.L. Coating of Nafion Membranes with Polyelectrolyte Multilayers to Achieve High Monovalent/Divalent Cation Electrodialysis Selectivities. *ACS Appl. Mater. Interfaces* **2015**, *7*, 6620–6628. [[CrossRef](#)] [[PubMed](#)]
22. Sheng, C.; Wijeratne, S.; Cheng, C.; Baker, G.L.; Bruening, M.L. Facilitated Ion Transport through Polyelectrolyte Multilayer Films Containing Metal-Binding Ligands. *J. Membr. Sci.* **2014**, *459*, 169–176. [[CrossRef](#)]
23. Porozhnyy, M.V.; Shkirskaia, S.A.; Butylskii, D.Y.; Dotsenko, V.V.; Safronova, E.Y.; Yaroslavtsev, A.B.; Deabate, S.; Huguet, P.; Nikonenko, V.V. Physicochemical and Electrochemical Characterization of Nafion-Type Membranes with Embedded Silica Nanoparticles: Effect of Functionalization. *Electrochim. Acta* **2021**, *370*, 137689. [[CrossRef](#)]
24. Patnaik, P.; Hossain, S.M.; Pal, S.; Sarkar, S.; Sharma, R.; Chatterjee, U. Controlling the Sub-Nano Ion Channels by Crosslinking in PVDF-Based Anion Exchange Membrane for Enhanced Mono/Bivalent Anion Permselectivity and Acid Reclamation. *J. Membr. Sci.* **2023**, *688*, 122105. [[CrossRef](#)]
25. Pacini, A.; Nitti, A.; Vitale, M.; Pasini, D. Poly(lactic)-Containing Hyperbranched Polymers through the CuAAC Polymerization of Aromatic AB<sub>2</sub> Monomers. *Int. J. Mol. Sci.* **2023**, *24*, 7620. [[CrossRef](#)] [[PubMed](#)]
26. Zabolotsky, V.; Utin, S.; Bepalov, A.; Strelkov, V. Modification of Asymmetric Bipolar Membranes by Functionalized Hyperbranched Polymers and Their Investigation during PH Correction of Diluted Electrolytes Solutions by Electrodialysis. *J. Membr. Sci.* **2015**, *494*, 188–195. [[CrossRef](#)]
27. Hsu, W.Y.; Gierke, T.D. Ion Transport and Clustering in Nafion Perfluorinated Membranes. *J. Membr. Sci.* **1983**, *13*, 307–326. [[CrossRef](#)]
28. Žagar, E.; Žigon, M. Aliphatic Hyperbranched Polyesters Based on 2,2-Bis(Methylol)Propionic Acid—Determination of Structure, Solution and Bulk Properties. *Prog. Polym. Sci.* **2011**, *36*, 53–88. [[CrossRef](#)]
29. Li, Y.S.; Zhao, T.S.; Yang, W.W. Measurements of Water Uptake and Transport Properties in Anion-Exchange Membranes. *Int. J. Hydrogen Energy* **2010**, *35*, 5656–5665. [[CrossRef](#)]

30. Karpenko, L.V.; Demina, O.A.; Dvorkina, G.A.; Parshikov, S.B.; Larchet, C.; Auclair, B.; Berezina, N.P. Comparative Study of Methods Used for the Determination of Electroconductivity of Ion-Exchange Membranes. *Russ. J. Electrochem.* **2001**, *37*, 287–293. [[CrossRef](#)]
31. Berezina, N.P.; Kononenko, N.A.; Dyomina, O.A.; Gnusin, N.P. Characterization of Ion-Exchange Membrane Materials: Properties vs Structure. *Adv. Colloid Interface Sci.* **2008**, *139*, 3–28. [[CrossRef](#)]
32. Falina, I.; Loza, N.; Loza, S.; Titskaya, E.; Romanyuk, N. Permselectivity of Cation Exchange Membranes Modified by Polyaniline. *Membranes* **2021**, *11*, 227. [[CrossRef](#)]
33. Zabolotsky, V.I.; Nikonenko, V.V. Effect of Structural Membrane Inhomogeneity on Transport Properties. *J. Membr. Sci.* **1993**, *79*, 181–198. [[CrossRef](#)]
34. Sharafan, M.V.; Zabolotsky, V.I. Study of Electric Mass Transfer Peculiarities in Electromembrane Systems by the Rotating Membrane Disk Method. *Desalination* **2014**, *343*, 194–197. [[CrossRef](#)]
35. Zabolotskii, V.I.; Sharafan, M.V.; Sheldeshov, N.V.; Lovtsov, E.G. Electric Mass Transport of Sodium Chloride through Cation-Exchange Membrane MK-40 in Dilute Sodium Chloride Solutions: A Rotating Membrane Disk Study. *Russ. J. Electrochem.* **2008**, *44*, 141–146. [[CrossRef](#)]
36. Zabolotskii, V.I.; Bugakov, V.V.; Sharafan, M.V.; Chermit, R.K. Transfer of Electrolyte Ions and Water Dissociation in Anion-Exchange Membranes under Intense Current Conditions. *Russ. J. Electrochem.* **2012**, *48*, 650–659. [[CrossRef](#)]
37. Zabolotsky, V.I.; Achoh, A.R.; Lebedev, K.A.; Melnikov, S.S. Permselectivity of Bilayered Ion-Exchange Membranes in Ternary Electrolyte. *J. Membr. Sci.* **2020**, *608*, 118152. [[CrossRef](#)]
38. Achoh, A.R.; Zabolotsky, V.I.; Lebedev, K.A.; Sharafan, M.V.; Yaroslavtsev, A.B. Electrochemical Properties and Selectivity of Bilayer Ion-Exchange Membranes in Ternary Solutions of Strong Electrolytes. *Membr. Membr. Technol.* **2021**, *3*, 52–71. [[CrossRef](#)]
39. Kononenko, N.A.; Loza, N.V.; Shkirskaia, S.A.; Falina, I.V.; Khanukaeva, D.Y. Influence of Conditions of Polyaniline Synthesis in Perfluorinated Membrane on Electrotransport Properties and Surface Morphology of Composites. *J. Solid State Electrochem.* **2015**, *19*, 2623–2631. [[CrossRef](#)]
40. Golubenko, D.V.; Yaroslavtsev, A.B. Effect of Current Density, Concentration of Ternary Electrolyte and Type of Cations on the Monovalent Ion Selectivity of Surface-Sulfonated Graft Anion-Exchange Membranes: Modelling and Experiment. *J. Membr. Sci.* **2021**, *635*, 119466. [[CrossRef](#)]
41. Zhang, Z.; Qiao, C.; Zhang, J.; Zhang, W.; Yin, J.; Wu, Z. Synthesis of Unimolecular Micelles with Incorporated Hyperbranched Boltorn H30 Polyester Modified with Hyperbranched Helical Poly(Phenyl Isocyanide) Chains and Their Enantioselective Crystallization Performance. *Macromol. Rapid Commun.* **2017**, *38*, 1700315. [[CrossRef](#)]
42. Yaroslavtsev, A.B.; Karavanova, Y.A.; Safronova, E.Y. Ionic Conductivity of Hybrid Membranes. *Pet. Chem.* **2011**, *51*, 473–479. [[CrossRef](#)]
43. Chintapalli, M.; Timachova, K.; Olson, K.R.; Mecham, S.J.; Devaux, D.; Desimone, J.M.; Balsara, N.P. Relationship between Conductivity, Ion Diffusion, and Transference Number in Perfluoropolyether Electrolytes. *Macromolecules* **2016**, *49*, 3508–3515. [[CrossRef](#)]
44. Kovalenko, A.V.; Nikonenko, V.V.; Chubyr, N.O.; Urtenov, M.K. Mathematical Modeling of Electrodialysis of a Dilute Solution with Accounting for Water Dissociation-Recombination Reactions. *Desalination* **2023**, *550*, 116398. [[CrossRef](#)]
45. Mikhaylin, S.; Nikonenko, V.; Pismenskaya, N.; Pourcelly, G.; Choi, S.; Kwon, H.J.; Han, J.; Bazinet, L. How Physico-Chemical and Surface Properties of Cation-Exchange Membrane Affect Membrane Scaling and Electroconvective Vortices: Influence on Performance of Electrodialysis with Pulsed Electric Field. *Desalination* **2016**, *393*, 102–114. [[CrossRef](#)]
46. Bondarev, D.; Melnikov, S.; Zabolotskiy, V. New Homogeneous and Bilayer Anion-Exchange Membranes Based on N,N-Diallyl-N,N-Dimethylammonium Chloride and Ethyl Methacrylate Copolymer. *J. Membr. Sci.* **2023**, *675*, 121510. [[CrossRef](#)]
47. Dukhin, S.S. Electrokinetic Phenomena of the Second Kind and Their Applications. *Adv. Colloid Interface Sci.* **1991**, *35*, 173–196. [[CrossRef](#)]
48. Nikonenko, V.V.; Mareev, S.A.; Pis'menskaya, N.D.; Uzdenova, A.M.; Kovalenko, A.V.; Urtenov, M.K.; Pourcelly, G. Effect of Electroconvection and Its Use in Intensifying the Mass Transfer in Electrodialysis (Review). *Russ. J. Electrochem.* **2017**, *53*, 1122–1144. [[CrossRef](#)]
49. Akberova, E.M.; Vasil'eva, V.I.; Zabolotsky, V.I.; Novak, L. Effect of the Sulfocation-Exchanger Dispersity on the Surface Morphology, Microrelief of Heterogeneous Membranes and Development of Electroconvection in Intense Current Modes. *J. Membr. Sci.* **2018**, *566*, 317–328. [[CrossRef](#)]
50. Rubinstein, I. Electroconvection at an Electrically Inhomogeneous Permselective Interface. *Phys. Fluids A* **1991**, *3*, 2301–2309. [[CrossRef](#)]
51. Simons, R. Strong Electric Field Effects on Proton Transfer between Membrane Bound Amines and Water. *Nature* **1979**, *280*, 824–826. [[CrossRef](#)]
52. Zabolotskii, V.I.; Shel, N.V.; Gnusin, N.P. Dissociation of Water Molecules in Systems with Ion-Exchange Membranes. *Russ. Chem. Rev.* **1988**, *57*, 801–808. [[CrossRef](#)]
53. Mishchuk, N.A.; Takhistov, P.V. Electroosmosis of the Second Kind. *Colloids Surf. A Physicochem. Eng. Asp.* **1995**, *95*, 119–131. [[CrossRef](#)]

54. Balster, J.; Yildirim, M.H.; Stamatialis, D.F.; Ibanez, R.; Lammertink, R.G.H.; Jordan, V.; Wessling, M. Morphology and Microtopology of Cation-Exchange Polymers and the Origin of the Overlimiting Current. *J. Phys. Chem. B* **2007**, *111*, 2152–2165. [[CrossRef](#)] [[PubMed](#)]
55. Nikonenko, V.V.; Kovalenko, A.V.; Urtenov, M.K.; Pismenskaya, N.D.; Han, J.; Sistas, P.; Pourcelly, G. Desalination at Overlimiting Currents: State-of-the-Art and Perspectives. *Desalination* **2014**, *342*, 85–106. [[CrossRef](#)]
56. Aritomi, T.; van den Boomgaard, T.; Strathmann, H. Current-Voltage Curve of a Bipolar Membrane at High Current Density. *Desalination* **1996**, *104*, 13–18. [[CrossRef](#)]
57. Balster, J.; Stamatialis, D.F.; Wessling, M. Electro-Catalytic Membrane Reactors and the Development of Bipolar Membrane Technology. *Chem. Eng. Process. Process Intensif.* **2004**, *43*, 1115–1127. [[CrossRef](#)]
58. Zabolotskii, V.I.; Nikonenko, V.V.; Korzhenko, N.M.; Seidov, R.R.; Urtenov, M.K. Mass Transfer of Salt Ions in an Electromembrane System with Violated Electroneutrality in the Diffusion Layer: The Effect of a Heterolytic Dissociation of Water. *Russ. J. Electrochem.* **2002**, *38*, 810–818. [[CrossRef](#)]
59. Melnikov, S.S.; Nosova, E.N.; Melnikova, E.D.; Zabolotsky, V.I. Reactive Separation of Inorganic and Organic Ions in Electrodialysis with Bilayer Membranes. *Sep. Purif. Technol.* **2021**, *268*, 118561. [[CrossRef](#)]
60. Sharafan, M.V.; Zabolotskii, V.I.; Bugakov, V.V. Electric Mass Transport through Homogeneous and Surface-Modified Heterogeneous Ion-Exchange Membranes at a Rotating Membrane Disk. *Russ. J. Electrochem.* **2009**, *45*, 1162–1169. [[CrossRef](#)]
61. Belashova, E.D.; Melnik, N.; Pismenskaya, N.D.; Shevtsova, K.; Nebavsky, A.; Lebedev, K.A.; Nikonenko, V.V. Overlimiting Mass Transfer through Cation-Exchange Membranes Modified by Nafion Film and Carbon Nanotubes. *Electrochim. Acta* **2012**, *59*, 412–423. [[CrossRef](#)]
62. Gil, V.; Porozhnyy, M.; Rybalkina, O.; Butylskii, D.; Pismenskaya, N. The Development of Electroconvection at the Surface of a Heterogeneous Cation-Exchange Membrane Modified with Perfluorosulfonic Acid Polymer Film Containing Titanium Oxide. *Membranes* **2020**, *10*, 125. [[CrossRef](#)]
63. Zyryanova, S.; Mareev, S.; Gil, V.; Korzhova, E.; Pismenskaya, N.; Sarapulova, V.; Rybalkina, O.; Boyko, E.; Larchet, C.; Dammak, L.; et al. How Electrical Heterogeneity Parameters of Ion-Exchange Membrane Surface Affect the Mass Transfer and Water Splitting Rate in Electrodialysis. *Int. J. Mol. Sci.* **2020**, *21*, 973. [[CrossRef](#)] [[PubMed](#)]
64. Titorova, V.D.; Moroz, I.A.; Mareev, S.A.; Pismenskaya, N.D.; Sabbatovskii, K.G.; Wang, Y.; Xu, T.; Nikonenko, V.V. How Bulk and Surface Properties of Sulfonated Cation-Exchange Membranes Response to Their Exposure to Electric Current during Electrodialysis of a Ca<sup>2+</sup> Containing Solution. *J. Membr. Sci.* **2022**, *644*, 120149. [[CrossRef](#)]
65. Nikonenko, V.V.; Zabolotskii, V.I.; Lebedev, K.A. Model for the Competitive Transport of Ions through Ion Exchange Membranes with a Modified Surface. *Russ. J. Electrochem.* **1996**, *32*, 234–236.
66. Kovalev, N.V.; Karpenko, T.V.; Sheldeshov, N.V.; Zabolotskii, V.I. Ion Transport through a Modified Heterogeneous Bipolar Membrane and Electromembrane Recovery of Sulfuric Acid and Sodium Hydroxide from a Sodium Sulfate Solution. *Membr. Membr. Technol.* **2020**, *2*, 391–398. [[CrossRef](#)]
67. Mareev, S.A.; Evdochenko, E.; Wessling, M.; Kozaderova, O.A.; Niftaliev, S.I.; Pismenskaya, N.D.; Nikonenko, V.V. A Comprehensive Mathematical Model of Water Splitting in Bipolar Membranes: Impact of the Spatial Distribution of Fixed Charges and Catalyst at Bipolar Junction. *J. Membr. Sci.* **2020**, *603*, 118010. [[CrossRef](#)]

**Disclaimer/Publisher’s Note:** The statements, opinions and data contained in all publications are solely those of the individual author(s) and contributor(s) and not of MDPI and/or the editor(s). MDPI and/or the editor(s) disclaim responsibility for any injury to people or property resulting from any ideas, methods, instructions or products referred to in the content.